Eur. Phys. J. D (2015) 69: 80
DOI: 10.1140/epjd/e2015-50641-7

THE EUROPEAN PHYSICAL JOURNAL D

Regular Article

Electron impact ionization of the gas-phase sorbitol*

Irina Chernyshova, Pavlo Markush[a], Anatoly Zavilopulo, and Otto Shpenik

Institute of Electron Physics, Ukrainian National Academy of Sciences, 21 Universitetska str., 88017 Uzhgorod, Ukraine

Received 29 August 2014 / Received in final form 29 December 2014
Published online 19 March 2015 –

Abstract. Ionization and dissociative ionization of the sorbitol molecule by electron impact have been studied using two different experimental methods. In the mass range of m/z = 10–190, the mass spectra of sorbitol were recorded at the ionizing electron energies of 70 and 30 eV. The ion yield curves for the fragment ions have been analyzed and the appearance energies of these ions have been determined. The relative total ionization cross section of the sorbitol molecule was measured using monoenergetic electron beam. Possible fragmentation pathways for the sorbitol molecule were proposed.

1 Introduction

Exceptional biological significance and large scale industrial uses of alcohol molecules gave a strong impetus to the electron impact investigation of these molecules. Another reason for studying them is that they can be found in the interstellar medium as well as in numerous planetary atmospheres [1,2]. Electron impact investigation of alcohol molecules can help to understand processes taking place at the biological systems irradiation [3–5]. A significant amount of data is available on the methanol (CH_3OH), ethanol (C_2H_5OH), propanol (C_3H_7OH), butanol (C_4H_9OH) and allyl alcohol (C_3H_5OH) [6–9], while polyatomic aliphatic alcohols included sorbitol ($C_6H_{14}O_6$) are less studied.

As a rule, at electron-molecule collisions first an unstable molecular ion is formed that decays spontaneously into a smaller ion and a neutral particle (atom or molecule) [10]. A number of experimental and theoretical works are devoted to studying ionization of the complex organic compounds [2,4,9]. However, in these works the main focus is put on obtaining the ionization energy (IE) of the parent molecule as well as the appearance energies (AE) of the fragment ions produced due to dissociative ionization. With regard to studying and analyzing the near-threshold behavior of the fragment ion yields, such data are significantly scarcer, while in case of the alcohol molecules they are not available at all.

Mass spectrometry is one of the most informative methods of studying the processes of direct and dissociative ionization. This method makes it possible to obtain not only the mass spectrum but the relative intensity for each dissociated fragment, as well as to measure the relative cross sections of both direct and dissociative ionization. In addition, the use of electron beam with high energy resolution allows the fine structure of the cross sections both in the near-threshold region and above it to be investigated.

In this work, the results on both relative total ionization cross section and dissociative electron-impact ionization cross sections for sorbitol are presented. The mass spectra were measured at the ionizing electron energies of 70 and 30 eV, the behavior of fragment ions in the energy range from the threshold up to 22 eV were also studied.

2 Experiment

The experiment was carried out by means of two different experimental techniques:

- a crossed electron-molecular beam method using a monopole mass spectrometer [11];
- a gas-filled cell method using a hypocycloidal electron spectrometer (HES) [12].

2.1 Monopole mass spectrometer

The molecular beam was produced by evaporating the substance under investigation using an effusive multichannel source of neutral particles. The molecular beam concentration in the region of interaction with the electron beam was not lower than 10^{11}–10^{12} cm^{-3} at the residual gas pressure in the vacuum chamber of 10^{-4} Pa. A MX 7304A monopole mass spectrometer with a modernized ion source [13] was used as the analytical instrument. This source enabled the electron beams of controlled energy (5–90 eV) to be obtained in the electron current stabilization mode at the current values of 0.03–0.3 mA and

* Contribution to the Topical Issue "Elementary Processes with Atoms and Molecules in Isolated and Aggregated States", edited by Friedrich Aumayr, Bratislav Marinkovic, Stefan Matejcik, John Tanis and Kurt H. Becker.

[a] e-mail: 1988.markus@gmail.com

with the energy resolution $\Delta E = 250$ meV (FWHM). The electron beam was produced via a heated tungsten filament. The ions produced by electron impact were extracted and focused into a beam using an ion lens and an extraction field. Thereafter the formed ion beam moved to the analyzer (mass filter) electrode area consisting of two oppositely disposed cylindrical and rectangular electrodes, where the ions were separated with respect to their mass-to-charge ratio (m/z) and detected by a secondary electron multiplier. The reliable control of the main parameters of the mass spectrometer was ensured by a PC that made it possible to measure, besides the mass spectra, energy dependences of the ion yield curves for the fragment ions in the energy range from the threshold up to 90 eV in the multiple scanning mode. The mass scale was calibrated using the Kr and Xe mass lines. The energy scale zero point as well as the energy spread of the electron beam were determined by measuring and analyzing the Kr atom ionization function. The experiment was carried out in two stages; at the first stage, the mass spectra of sorbitol were recorded, while at the second stage, the ion yield curves for the fragment ions were measured in the 9–22 eV energy range.

2.2 Hypocycloidal electron spectrometer

Additional experiments were carried out using a hypocycloidal electron spectrometer [12] with a gas-filled cell to obtain further information on sorbitol molecule ionization by electron impact. This instrument consists of two identical successive hypocycloidal electron monochromators (HEMs) [14]: one of them operating as a monochromator, the second being a scattered-electron analyzer. They are separated by a gas-filled cell that serves as a collision chamber. We chose the HEM to form an electron beam because it provides beams of rather high density and small electron-energy spread. The complete collection of electrons was ensured by an electron collector in a form of a deep Faraday cylinder. The best HEM energy resolution in these measurements was $\Delta E_{1/2} = 100$ meV (FWHM) at an electron current of 10–20 nA. The scattered-electron analyzer was not used in these experiments. It is applied usually for studying the excitation processes in atoms and molecules (see, for instance, [15]).

The gas-phase target was produced in a reservoir in a form of a hollow stainless-steel cylinder heated resistively to desired temperature (about 326 K), at which no structural changes take place in the sorbitol molecule ($T_m = 368$ K) [16]. The spectrometer temperature was maintained 30 K higher than that of the reservoir to avoid sorbitol condensation on the HES elements. The residual gas pressure in the vacuum chamber under operating conditions did not exceed 2.5×10^{-4} Pa. The electrons were accelerated by a potential difference applied between the cathode and the collision chamber. The energy scale calibration was carried out with respect to the shift of the electron beam current-voltage dependence at the collector. The ion current was measured using a detector placed inside the collision chamber to which a negative potential of 6 V was applied to collect all the ions produced. The measured ion current value was 0.1 pA at the electron beam current of 90 nA.

It is well known that dehydration (the loss of the water molecule) plays an important role in sugar alcohols evaporation even at room temperature [17]. In order to see how the ion current background component from the water molecule ions varies, the temperature of the reservoir was raised gradually (for about three hours) and the ion signal was measured permanently in the entire incident electron energy range. As it was expected, the ion signal first increased, then, after reaching the temperature of 310 K, it fell down and remained constant. The reservoir temperature was raised again to 326 K to achieve a high signal to noise ratio. Finally the background signal measured at 310 K was subtracted from that recorded at 326 K to obtain the valid signal. The signal recording and measurement parameter controlling were automated using special software developed by us.

3 Results and discussion

It is well known [18] that ionization energy determination in organic compounds faces a number of difficulties. The precise determination of ionization energy is strongly affected by such factors as the low value of the ionization cross section near the threshold, the slow rise of the ionization cross section, the electron beam energy resolution and the energy scale calibration accuracy. The ionization energies of molecules and the appearance energies of fragment ions are usually obtained by fitting the ion yield curves near the threshold to the Wannier law function [19], which can minimize some of the above factors [20].

The sorbitol mass spectra were measured at the temperature of 390 K and the ionizing electron energies of 70 and 30 eV, the behavior of the ion yield curves for the fragment ions was investigated in the energy range from the threshold up to 22 eV. The relative total ionization cross section of sorbitol was measured using an electron beam with high energy resolution.

Sorbitol (1,2,3,4,5,6-hexanehexol – $C_6H_{14}O_6$) is one of the hexitol alcohols. Hexitols – hexahydric aliphatic alcohols $HOCH_2(CHOH)_4CH_2OH$ – consist of six OH groups and four asymmetric carbon atoms forming two pairs of identical structure [21].

3.1 Mass spectra

Mass spectra measured at the ionizing electron energies of 70 and 30 eV can be seen in Figure 1. As seen, no molecular ion peak M^+ (m/z 182) is observed in these spectra, and such pattern is typical for polyatomic alcohols [18]. This is the evidence for the instability of the sorbitol molecule that decays immediately at ionization. The two dominant fragmentation pathways of the sorbitol molecular ion are the C–C bond breaks and the rearrangement processes associated with the water or formaldehyde

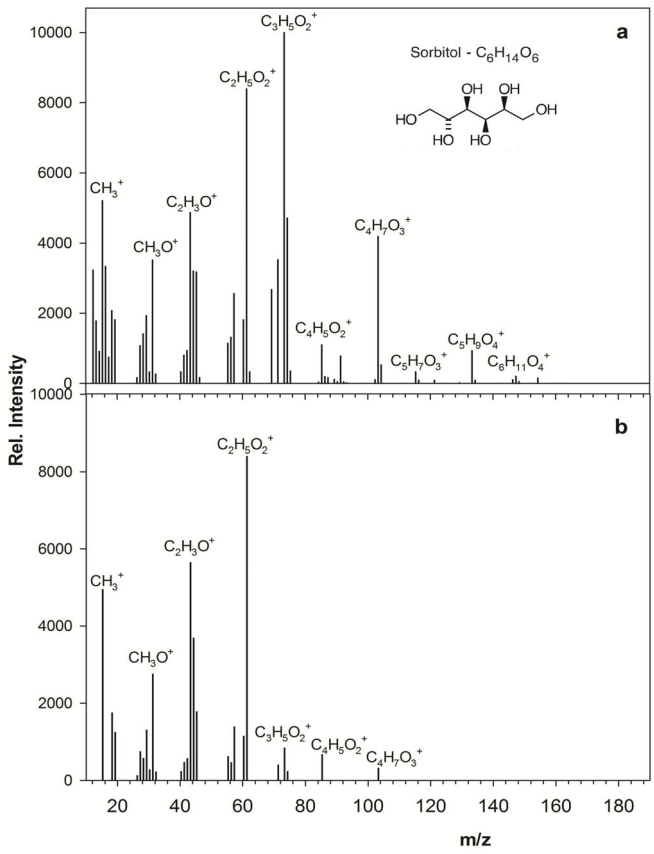

Fig. 1. The sorbitol mass spectra recorded at $E_i = 70$ eV (a) and 30 eV (b), $T = 390$ K.

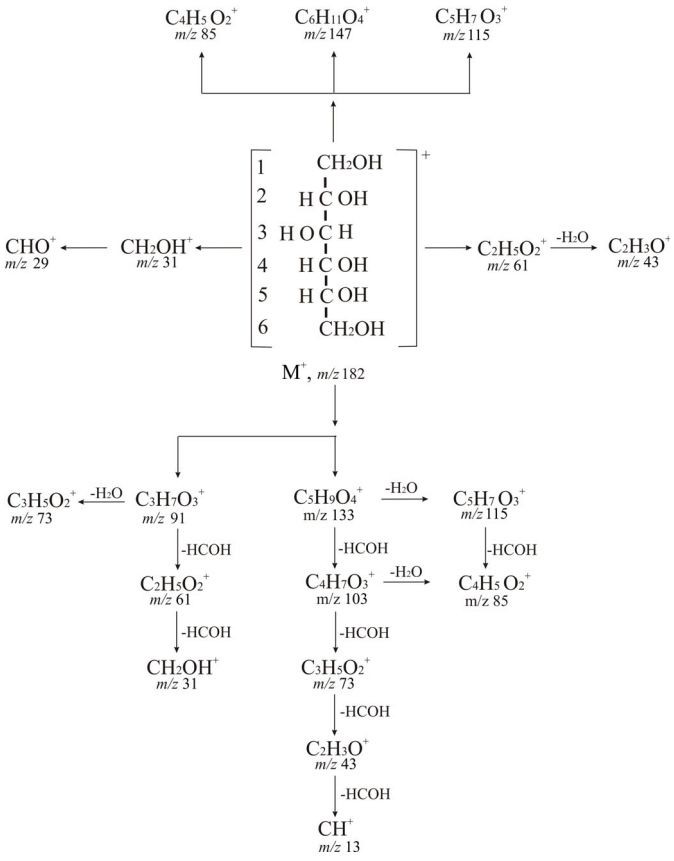

Fig. 2. Proposed fragmentation pathways for the sorbitol molecule.

molecules elimination. Furthermore, besides the molecular ion M^+, certain fragment hydroxyl ions can also be exposed to dehydration. It is important to note that the hydrogen atom detached together with the hydroxyl group can be captured from different positions.

In the mass spectrum recorded at $E_i = 70$ eV, the ions with m/z 73, 61, 15, 43, 103, 31 have the most intense peaks (Fig. 1a). Four of them at $m/z = 31, 43, 61, 73$ are characteristic for the alcohol molecules [18]. Besides these ion peaks, a series of peaks at $m/z = 133, 103, 73, 43$ and 13 can be observed, in addition, the mass difference between them is exactly 30. It is the evidence that they may be formed as a result of the C–C bond break with the loss of the CH_2O fragment (m/z 30). The peak intensities of these fragment ions are related as follows: m/z $133 < 103 < 73 > 43 > 13$ (Fig. 1a). It is worth noting that the ion peak pairs at $m/z = 103$, $m/z = 43$, and $m/z = 133$, $m/z = 13$ have almost the same intensities. The explanation is that these fragment ions have the same probability of formation due to the symmetric structure of the molecule under study.

The fragment ions with m/z 31, 73 and 85 can be produced as a result of the secondary rearrangement processes via a four-member transition state. Formation of the ion with m/z 45 can be explained by the rearrangement processes via a six-member transition state. Taking into account the above, the following fragmentation scheme for the sorbitol molecule has been suggested (see Fig. 2).

In the mass spectrum, the $C_6H_{11}O_4^+$ fragment ion $[M–35]^+$ with m/z 147 has the largest mass, it is produced due to the simultaneous elimination of water molecule and hydroxyl group. The detachment of the hydrogen atom from the molecular ion with water molecule formation occurs via a four-member transition state [22]. The $C_6H_{11}O_4^+$ ion peak has a relatively low intensity, and this may be explained by its instability under the electron impact. This ion fragmentation with the loss of water (m/z 18) and C_2H_2 (m/z 26) ethylene molecules results in the formation of the $C_4H_7O_3^+$ ion (m/z 103).

The C_1–C_2 bond break in the molecular ion with water molecule elimination leads to the formation of the $C_5H_9O_4^+$ ion with m/z 133. However, this fragment ion has an excess energy enough to cause the loss either of the water or the formaldehyde molecule resulting in the $C_5H_7O_3^+$ (m/z 115) and $C_4H_7O_3^+$ (m/z 103) ion formation.

The simultaneous detachment of the CH_2OH molecular fragment from one end of the M^+ parent ion (i.e. the break of the C_1–C_2 bond or the C_5–C_6 carbon skeleton) as well as that of the two water molecules can lead to the formation of the $C_5H_7O_3^+$ ion $[M–67]^+$ with m/z 115.

The C_4–C_5 bond break with the water molecule elimination results in the formation of the $C_4H_7O_3^+$ ion

$[M–79]^+$ (m/z 103) that contains four carbon atoms in the chain.

The dissociation of the C_3–C_4 bond may lead to the formation of two complementary $C_3H_7O_3^+$ ions with m/z 91 having low intensity in the mass spectrum measured at 70 eV ionizing electron energy. These fragments have the excess energy that may cause the water or CH_2O (m/z 30) formaldehyde molecule detachment resulting in the secondary $C_3H_5O_2^+$ (m/z 73) or $C_2H_5O_2^+$ (m/z 61) ions formation. These ions have larger peak intensity than that produced due to the primary dissociation of the molecular ion (Fig. 1a).

It should be noted that formation of the $C_2H_5O_2^+$ fragment ion (m/z 61) with two carbon atoms can also occur via the C_2–C_3 bond break in the M^+ molecular ion. Further dehydration of this ion leads to the formation of the $C_2H_3O^+$ ion with m/z 43. Elimination of the formaldehyde molecule (CH_2O) in case of the $C_2H_5O_2^+$ ion results in the CH_3O^+ ion formation with m/z 31. This ion may also be produced as a result of the C_1–C_2 bond break when the charge localization occurs at one of the carbon atoms of the molecular ion. In addition, the fragment ions are more likely to lose heavier radicals.

As seen, in the mass spectrum measured at $E_i = 30$ eV the fragment ions with m/z 91 and those above m/z 103 are not present as well as the m/z 73 and 103 peaks have low intensity which being the main differences between the two spectra. This can be explained by the fact that at the ionizing electron energy of 70 eV the $C_3H_5O_2^+$ ion (m/z 73) has the highest probability of formation, while at the ionizing electron energy of 30 eV the $C_2H_5O_2^+$ ion (m/z 61) is produced more likely. The high intensity of the ion peaks at m/z 61, 15, 43 and 31 in the mass spectra indicates that they can be produced with equal probability due to direct and rearrangement processes [23].

The temperature dependences of the ion yield for the fragment ions with m/z 15, 18, 31, 43, 61 and 103 were measured in the temperature range of 300–440 K to find the optimal temperature for measuring the mass spectra. It has been found that all the fragment ions have the maximum ion yield in the temperature range of 380–420 K.

3.2 Energy dependences

The energy dependences of the ion yield for CH_3^+ (m/z 15), CHO^+ (m/z 29), CH_2OH^+ (m/z 31), $C_2H_3O^+$ (m/z 43), $C_2H_5O_2^+$ (m/z 61), $C_3H_5O_2^+$ (m/z 73), $C_4H_5O_2^+$ (m/z 85), $C_3H_7O_3^+$ (m/z 91), $C_5H_7O_3^+$ (m/z 115) and $C_5H_9O_4^+$ (m/z 133) fragment ions have also been measured in the energy range from the threshold to 22 eV (see Fig. 3). The appearance energies of these fragments have been determined by using the Wannier threshold law. For some fragment ions (m/z 31, 43 and 133) the appearance energies were not possible to obtain by Wannier threshold law because of the high error value. In case of these ions the linear extrapolation method was applied. The obtained appearance energies are presented in Table 1.

As our studies have shown, the behavior of the energy dependences in the near-threshold (below 14 eV) region is not the same, i.e. a smooth cross section increase is observed for the ionic fragments with m/z 43, 61, 73 and 85; a weak maximum appears for m/z 29, 31, 115 and 133 and, finally, for the ionic fragment with m/z 15 and 91 a more intense ion yield is observed in this energy region as compared to the other ionic fragments.

Table 1. Appearance energies and relative intensities of the fragment ions obtained from the mass spectrometric measurements performed at $E_i = 70$ and 30 eV.

Ion	Ion mass m/z	Relative intensity %		Appearance energy (E_{AE}) ±0.25 eV
		30 eV	70 eV	
M^+	182			
$C_5H_9O_4^+$	133		9.6	9.5
$C_5H_7O_3^+$	115		3.5	11.68
$C_4H_7O_3^+$	103	4	42	9.9
$C_3H_7O_3^+$	91		8.2	10.3
$C_4H_5O_2^+$	85	8	11.2	11.57
$C_3H_5O_2^+$	73	10	100	10.3
$C_2H_5O_2^+$	61	100	84.5	10.44
$C_2H_3O^+$	43	67	49	10.11
CH_3O^+	31	33	35	10.26
CHO^+	29		19.8	10.6
CH_3^+	15	58	52	9.8

The energy dependences of the ion yield of the CHO^+ (m/z 29) and CH_2OH^+ (m/z 31) ions, the members of the aldehyde group, show similarity, i.e. their appearance energies are also close to each other (10.6 and 10.26 eV, respectively). As seen, the energy dependences of these ions exhibit a weak maximum in the near-threshold energy region followed by a slow rise with a maximum above 20 eV. The appearance of the weak maximum in the near-threshold energy region can be attributed to the contribution of the vibrational excitation of the Rydberg states converging to the excited state of ion. This assumption is based on the result of work [24], in which the CH_2O^+ ion (m/z 30) was investigated, and the Rydberg states were found at 11.456 eV and 12.479 eV, respectively. The Rydberg series converging to the second excited state at 15.84 eV are close to the features observed in the ion yield curves.

We would like to draw attention to the ion yield curve of the fragment ion with m/z 15, whose appearance energy is 9.8 eV. This value coincides well with the result of [25,26]. Two distinct breaks can be observed in the near-threshold energy region at 10.75 and 11.56 eV which being followed by a sharp curve increase. This curve increase was also observed in the relative photoionization cross section of CH_3 [27]. Authors of this work have explained it by the contribution of autoionization states. The energy dependence exhibits two distinct features in the energy ranges of 12–14 and 15–17 eV. The energy positions of these breaks coincide well with the results of work [26]. The ion yield curve of the CH_3^+ (m/z 15) ion has some features (at the energies of 15.09 and 15.58 eV) that can be related to the CH_2^+ and CH^+ ion formation [16,27]. The curve increase

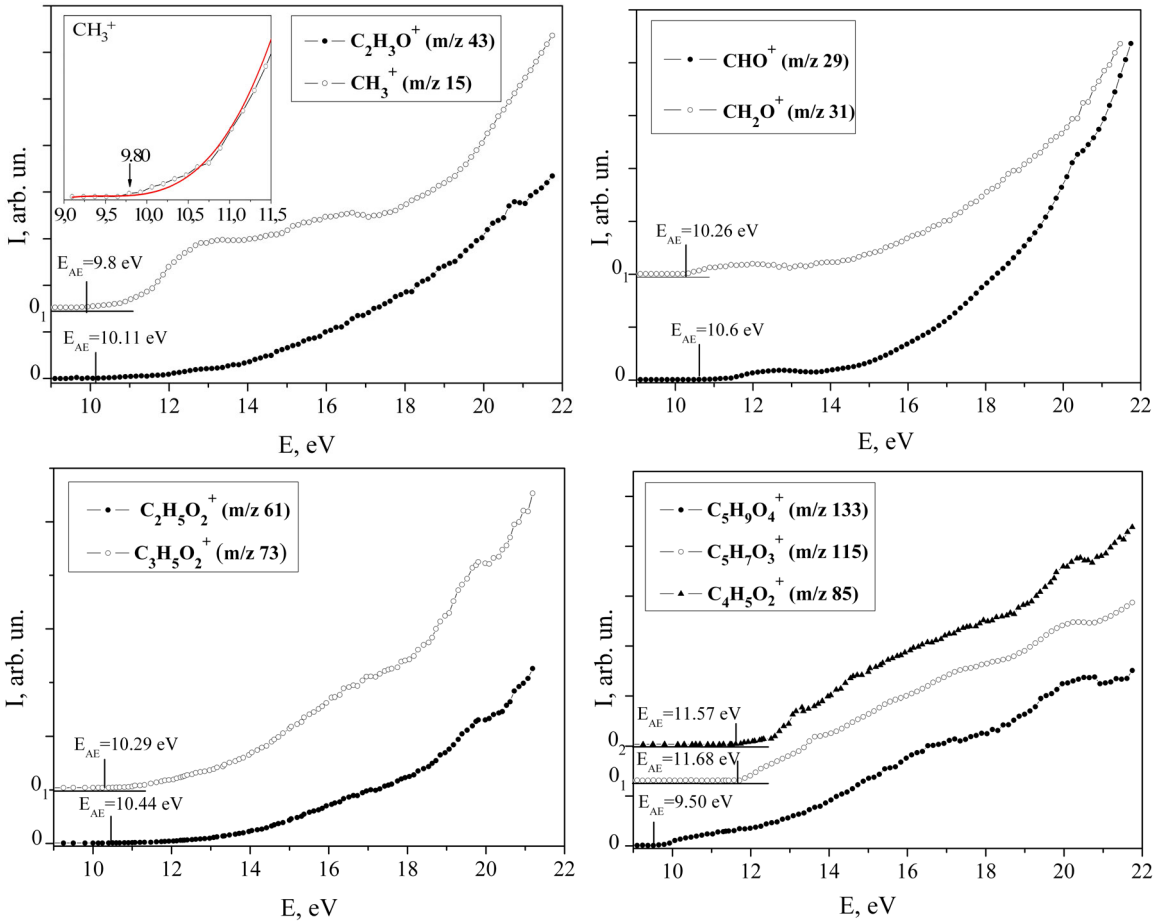

Fig. 3. The ion yield curves for the fragment ions measured in the electron energy range from the threshold to 22 eV; inset shows the enlarged near threshold energy region of the m/z 15 ion with the fitting procedure used to determine the appearance energy (0_1 and 0_2 indicate the zero point for the particular ion on the y-axis).

above 19 eV can be attributed to the contribution of hydrogen ionic fragment [28–30].

A maximum near 20 eV is observed in all the curves which varying dependent on the fragment ion mass. This phenomenon can be explained by the dissociation of the water molecule that decays into the OH^+, O^+, H_2^+ fragments having the appearance energies 18.1 eV, 19.0 eV and 20.7 eV [31], respectively. This maximum does not appear in the ion yield curve measured for the CH_3^+ ion with m/z 15 that also confirms our assumption.

All the curves (except for $m/z = 15$) have a characteristic feature in a form of a maximum at the energy about 17.5 eV. The appearance of this feature can be explained by the dissociative excitation of the OH-group [32].

The measured curves for the ions produced as a result of the C_3–C_4 bond break in the initial molecule differ slightly from the other ones. The appearance energies for the $C_3H_7O_3^+$ (m/z 91), $C_3H_5O_2^+$ (m/z 73) and $C_2H_5O_2^+$ (m/z 61) ions listed in Table 1 indicate that the C_3–C_4 bond is the first to be broken at the sorbitol molecule dissociation. The behavior of the curves measured for the ions with m/z 61 and m/z 73 demonstrate that formation of the $C_3H_5O_2^+$ ion is energetically more efficient than that of the $C_2H_5O_2^+$ ion. The lower appearance energy of the $C_3H_5O_2^+$ ion and its higher peak intensity in the $E_i = 70$ eV mass-spectrum also confirm our assumption.

3.3 Total ionization cross section of the sorbitol molecule

The energy dependence of the total ionization cross section of the sorbitol molecule measured using the HES is shown in Figure 4. This is a relative cross section since the construction of our experimental technique made not possible the measurement of the gas pressure in the collision chamber required to determine the absolute value of the cross section. The measured total ionization cross section represents the sum of the parent molecular ion production cross section and those for all ionic fragments. As seen, the curve has a sharp rise near the threshold as well as features in a form of breaks (slope increase or decrease). The increase of slope in the measured curve is primarily due to the direct ionization of the sorbitol molecule, but it may also result from the formation of fragments due to dissociation. A relative decrease of the slope indicates

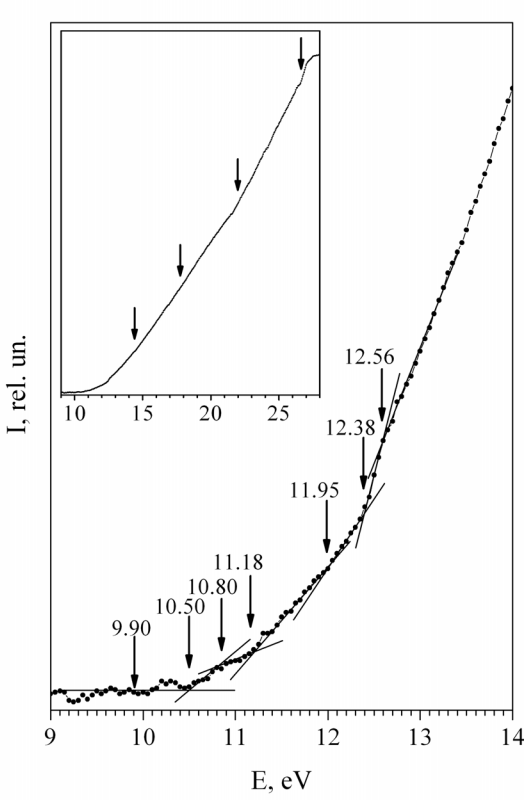

Fig. 4. Energy dependence of the total ionization cross section of the sorbitol molecule measured in the energy range of 9–14; inset shows the whole measurement range (arrows indicate the features energy positions).

fragmentation or predissociation of the parent ion [27]. The ionization energy of the gas phase sorbitol was determined to be 9.90 ± 0.05 eV using the Wannier threshold law. This value is in a good agreement with the appearance energy of CH_3^+ (m/z 15) obtained in the mass spectrometric experiment. It indicates that ionization of the CH_3 molecule occurs first at the 326 K temperature. It is worth noting that in the NIST database [16] no data on the electron-impact sorbitol molecule ionization energy are available.

Breaks can be observed in the measured curve at the 10.5, 10.8, 11.18, 11.95, 12.38, 12.56, 14.40, 17.78, 22.02 and 26.64 eV energies (indicated by arrows). The energies of these features were determined by approximating the measured curve by a series of linear segments whose intersection points reflect the onset (the appearance energies) of new ionization processes [33]. Taking into account the intensity of the ion peaks in the mass spectrum and their appearance energies, we assume that the breaks at 10.5, 10.8 and 11.95 eV correspond to the $C_2H_5O_2^+$, CHO^+ and C_5H_7 O_3^+ ions, respectively (see Tab. 1). After the ionization threshold a weak feature can be observed whose energy position agrees well with the appearance energies of fragment ions with m/z 31 (10.26 eV), m/z 73 (10.3 eV) and m/z 91 (10.3 eV). Two breaks at the 17.78, 26.64 eV energies were identified as corresponding to the appearance energies of the OH^+ (18.08 eV) and O^+ (26.5 eV) fragment ions [16].

4 Conclusions

The mass spectra of the sorbitol molecule have been recorded at different ionizing electron energies using the monopole mass spectrometer. The ion yield curves for the most intense fragment ions have been measured. The appearance energies of the fragment ions have also been determined. It has been found that sorbitol molecule electron impact dissociation occurs primarily via the break of the C_3–C_4 bond in the carbon skeleton resulting in the formation of fragments with high intensity. Fragmentation pathways for the sorbitol molecule have also been proposed.

The relative total ionization cross section for the sorbitol molecule has been measured for the first time using the HES with a gas filled cell. The ionization energy of the gas phase sorbitol was determined to be 9.90 ± 0.05 eV.

The authors would like to thank L.G. Romanova for her help in analyzing the results.

References

1. N.M. Bazhin, Sorosovsky Obrazovatelny Zhurnal **6**, 52 (2000)
2. F. Bell, Q.N. Ruan, A. Golan, P.R. Horn, M. Ahmed, S.R. Leone, M. Head-Gordon, J. Am. Chem. Soc. **135**, 14229 (2013)
3. F. Wang, J. Mol. Struct. (Theochem) **678**, 105 (2004)
4. D.A. Erwin, J.A. Kunc, J. Appl. Phys. **103**, 064906 (2008)
5. J.M. Heller Jr., R.D. Birkhoff, M.W. Williams, L.R. Painter, Radiat. Res. **52**, 25 (1972)
6. J.E. Hudson, M.L. Hamilton, C. Vallance, P.W. Harland, Phys. Chem. Chem. Phys. **5**, 3162 (2003)
7. S.K. Srivastava, E. Krishnakumar, A.F. Fucaloro, T. van Note, J. Geophys. Res. **101**, 26155 (1996)
8. R. Rejoub, C.D. Morton, B.G. Lindsay, R.F. Stebbings, J. Chem. Phys. **118**, 1756 (2003)
9. A.N. Zavilopulo, F.F. Chipev, L.M. Kokhtych, Nucl. Instrum. Methods Phys. Res. B **233**, 302 (2005)
10. J. Gross, *Mass Spectrometry* (Springer-Verlag, Berlin, Heidelberg, 2011)
11. A.N. Zavilopulo, M.I. Mykyta, A.N. Mylymko, O.B. Shpenik, Techn. Phys. **58**, 1251 (2013)
12. J.E. Kontros, L. Szoter, I.V. Chernyshova, O.B. Shpenik, J. Phys. B **35**, 2195 (2002)
13. A.N. Zavilopulo, O.B. Shpenik, P.P. Markush, M.I. Mykyta, Techn. Phys. Lett. **40**, 13 (2014)
14. M.I. Romanyuk, O.B. Shpenik, Meas. Sci. Technol. **5**, 239 (1994)
15. I.V. Chernyshova, E.E. Kontros, P.P. Markus, O.B. Shpenik, Opt. Spectrosc. **113**, 5 (2012)
16. NIST Standard Reference Database, http://www.nist.gov/srd/upload/REFPROP8_manua3.htm
17. M. Nimlos, S. Blanksby, X. Qian, M. Himmel, D. Johnson, J. Phys. Chem. A **110**, 6145 (2006)

18. A.T. Lebedev, *Mass-spectrometriya v organicheskoi khimii* (BINOM. Laboratoriya znanii, Moscow, 2003)
19. G.H. Wannier, Phys. Rev. **100**, 1180 (1955)
20. M. Stano, S. Matejcik, J.D. Skalny, T.D. Mark, J. Phys. B **36**, 261 (2003)
21. Wei Yan, Galen J. Suppes, J. Chem. Eng. Data **53**, 2033 (2008)
22. N.S. Vulfson, V.G. Zaikin, A.I. Mikaya, in *Mass-spectrometriya Organicheskih Soedinenii*, edited by V.I. Kozlova (Khimiya, Moscow, 1986)
23. I.G. Zenkevich, B.V. Ioffe, in *Interpretaziya Mass-spectrov Organicheskih Soedinenii*, edited by B.V. Ioffe (Khimiya, Leningrad, 1986)
24. P.M. Guyon, W.A. Chupka, J. Berkowitz, J. Chem. Phys. **64**, 1419 (1976)
25. F.P. Lossing, G.P. Semeluk, Can. J. Chem. **48**, 955 (1970)
26. C.E. Melton, W.H. Hamil, J. Chem. Phys. **41**, 3464 (1964)
27. W.A. Chupka, C. Lifshitz, J. Chem. Phys. **48**, 1109 (1968)
28. C.Y.R. Wu, D.L. Judge, J. Chem. Phys. **75**, 172 (1981)
29. K. Gluch, P. Sheier, W. Schustereder, T. Tepnual, L. Feketeova, C. Mair, S. Matt-Leubner, A. Stamatovic, T.D. Mark, Int. J. Mass Spectrom. **228**, 307 (2003)
30. M. Ziolkowski, A. Vikar, M.L. Mayes, A. Bencsura, G. Lendvay, G.C. Schatz, J. Chem. Phys. **137**, 22A510 (2012)
31. Y. Itikawa, N. Mason, J. Phys. Chem. Ref. Data **34**, 1 (2005)
32. H.P. Pritchard, V. McKoy, M.A.P. Lima, Phys. Rev. A **41**, 546 (1990)
33. W. Rosinger, M. Grade, W. Hirschwald, Int. J. Mass. Spectrom. Ion Phys. **47**, 239 (1983)